Article

Influence of Leachate and Nitrifying Bacteria on Photosynthetic Biogas Upgrading in a Two-Stage System

Luis Fernando Saldarriaga [1,2], Fernando Almenglo [1,*], Domingo Cantero [1] and Martín Ramírez [1]

1   Departamento de Ingeniería Química y Tecnología de Alimentos, Instituto de Investigación Vitivinícola y groalimentaria (IVAGRO), Universidad de Cadiz, 11510 Puerto Real, Spain; luissaldarriaga@mail.uniatlantico.edu.co (L.F.S.); domingo.cantero@uca.es (D.C.); martin.ramirez@uca.es (M.R.)
2   Departamento de Química, Universidad del Atlántico, Carrera 30 Número 8-49, Puerto Colombia 081001, Colombia
*   Correspondence: fernando.almenglo@uca.es; Tel.: +34-956-01-6864

Abstract: Photosynthetic biogas upgrading using two-stage systems allows the absorption of carbon dioxide (CO_2) in an absorption unit and its subsequent assimilation by microalgae. The production of microalgae requires large amounts of nutrients, thus making scale-up difficult and reducing economic feasibility. The photosynthetic process produces oxygen (O_2) (1 mol per mol of CO_2 consumed), which can be desorbed into purified biogas. Two-stage systems reduce its impact but do not eliminate it. In this study, we test the use of landfill leachate as a nutrient source and propose a viable and economical strategy for reducing the O_2 concentration. First, the liquid/gas (L/G) ratio and flow mode of the absorber were optimized for 20% and 40% CO_2 with COMBO medium, then landfill leachate was used as a nutrient source. Finally, the system was inoculated with nitrifying bacteria. Leachate was found to be suitable as a nutrient source and to result in a significant improvement in CO_2 absorption, with outlet concentrations of 0.01% and 0.6% for 20% and 40% CO_2, respectively, being obtained. The use of nitrifying bacteria allowed a reduction in dissolved oxygen (DO) concentration, although it also resulted in a lower pH, thus making CO_2 uptake slightly more difficult.

Keywords: photobioreactor; biogas upgrading; carbon dioxide; ammonia removal; biomethane; gas-liquid ratio; leachate; microalgae

1. Introduction

The use of biogas as a renewable energy source is strongly encouraged by international organizations and states. In this sense, the European Union has established an objective of reducing total greenhouse gas emissions by between 80% and 95% compared to 1990 [1]. Within the intermediate objectives in the framework on climate and energy for 2030, an estimated reduction in these emissions of at least 40% has been proposed [1]. In its report "A roadmap for moving to a competitive low carbon economy in 2050", the EU has established a target of an 80% reduction in emissions by 2050 [2]. Methane (CH_4) and carbon dioxide (CO_2) are the main gases present in biogas, with the potential effect of CH_4 on global warming being 24.5 times higher than that of CO_2. To obtain biomethane, according to the standard specifications of each region or country, biogas must be purified to eliminate minor compounds and then upgraded to vary the methane content [2].

The upgrading of biogas mainly reduces the CO_2 content, which is performed using physical, chemical and/or biological processes [3,4]. Of these, CO_2 assimilation by microalgae is a rapidly growing technology. The photosynthetic upgrading of biogas can be achieved by using one-stage [5,6] or two-stage systems [7–10]. In one-stage systems, the biogas is fed into a photobioreactor, where CO_2 is absorbed and assimilated by microalgae as a carbon source. In these systems, the oxygen (O_2) produced during photosynthesis can increase in concentration in the outlet biogas stream, with the CO_2 consumed mostly

being replaced by O_2 [10,11]. Two-stage systems contain an absorption unit (packed column, spray column, bubble column, etc.) and a photobioreactor. The most common photobioreactors used in two-stage systems are high-rate algal ponds (HRAP) [7,8] and tubular [9] and bubble columns [10]. The use of two-stage systems reduces the impact of the O_2 generated by photosynthesis as these systems use a CO_2 absorption unit, in which the CO_2 is transferred from the gas phase to the liquid phase, and the liquid phase is regenerated (biological assimilation of CO_2) in the photobioreactor [7,8,10]. Although the use of a two-stage system reduces the impact of the O_2 generated, photobioreactors are generally open to the environment or are bubbled with air. For this reason, the liquid effluent that returns to the absorption column is in equilibrium with the air, thus meaning that the dissolved oxygen (DO) can be desorbed in the biogas outlet stream. The symbiotic culture of microalgae and nitrifying bacteria is an interesting option to reduce the DO concentration, thereby reducing O_2 inhibition of microalgae growth and O_2 desorption in the CO_2 absorption unit. In this way, the O_2 generated by microalgal metabolism and the ammonium (NH_4^+) present in wastewater or leachate can support the growth of bacteria and the oxidation of NH_4^+ to nitrate (NO_3^-) and/or nitrite (NO_2^-), which can be used by microalgae [12–14]. Although nitrifying bacterial growth can suffer photoinhibition [15], symbiotic culture is nevertheless an interesting option to improve this technology. Packed columns, in which the packing material can be Rasching rings, polyurethane foam [16] or Pall rings [17], amongst others, are usually used as the absorption unit as the use of packing materials provides a greater contact surface area between the phases (gas and liquid), thus improving mass transfer [18] and allowing the development of bacterial biofilms.

In order for microalgae to carry out all their metabolic processes, an adequate supply of nutrients is essential. In addition to the main nutrients (CO_2, H_2O and light), other basic nutrients, such as nitrogen, phosphorus, magnesium, iron, and sulfur, etc., are also required [19]. Indeed, microalgae need large amounts of nutrients or fertilizers [20]. This has a direct effect on the profitability of any processes that involve the production of microalgae [21]. One alternative to the use of synthetic media may be the use of wastewater [11,22] or landfill leachate [23,24], especially those from agro-industrial waste and landfill leachate, which are rich in nitrogen and phosphorus [21,25]. The recovery of nutrients from leachate using microalgae has two clear advantages: firstly, they act as a nutrient carrier at a very low cost, and secondly, the positive impact on the environment by avoiding contamination and unwanted eutrophication processes.

This study aimed to describe the impact of landfill leachate as a source of nutrients and the use of a culture of nitrifying bacteria on the efficiency of a two-stage system for biogas upgrading. The two-stage system comprised a packed column with Rasching rings as the absorption unit and a bubble column as the photobioreactor. The effect of the liquid:gas ratio (L/G) in the absorption column was evaluated initially, then the nutrient source was replaced by landfill leachate. Finally, a culture of nitrifying bacteria was inoculated. These experiments allowed us to optimize the absorption column, verify the compatibility of nitrifying bacteria with the microalgae to obtain a biogas with a lower O_2 concentration, and verify the compatibility of these microorganisms with the use of landfill leachate as a nutrient source.

2. Materials and Methods

2.1. Experimental Set-Up

A schematic diagram of the two-stage system is shown in Figure 1. The bubble column photobioreactor was made of transparent polymethyl methacrylate (PlásticosFerplast S.L., Barcelona, Spain). The working volume was 55 L, the inner diameter was 19.4 cm and the total height was 205 cm. A stone air diffuser (15 cm) was used for aeration. A continuous flow of air enriched with CO_2 (3%) was fed into the photobioreactor (0.035 vvm), when required, for growth or maintenance of the microalgae. A mass flow controller (F-201 CV, Bronkhorst High-Tech B.V., Ruurlo, TheNetherlands) was used to fix the inlet CO_2 concentration and a variable area flow meter (FR2A12BVBN, Key Instruments, Tevose, PA,

USA) was used to measure the air flow rate. The pH and DO were monitored (Multimeter M44, CrisonIntruments S.A., Barcelona, Spain). The photobioreactor was illuminated with 2 LED panels (120 × 60 cm, 72W, 2880–3200, Lifud, Shenzhen, China) with a photoperiod of 24:0 light:dark cycles and an average surface irradiance of 126 µmol m^{-2} s^{-1}. The temperature was kept constant (20 ± 1 °C) by recirculating the culture through a thermostatic bath (RA-8 alpha, LAUDA, Lauda-Königshofen, Germany). The absorption unit was made of transparent PVC (inlet diameter 2.84 cm) (Agruquero Thermoplastics S.L., Pinto, Spain) packed with Rasching glass rings (diameter 5 mm). The working volume was 0.8 L, with a height:diameter (H:D) ratio of 44. The absorption unit was fed with substitute biogas (mixture of CO_2 and N_2) at a constant flow rate of 0.6 L h^{-1}. The substitute biogas was fed from Tedlar® Air Sample Bags (50 L, 232-50, SKC, Eighty Four, PA, USA) using a peristaltic pump (7544-30, Cole Parmer Instruments Company LLC., Vernon Hills, IL, USA). The system was controlled and monitored using LabVIEW^{TM} 2015 (v.15.0f2, National Instruments^{TM}, Austin, TX, USA) with cDAQ Chassis (NO-9184) and modules for analog input (NI-9208) and a digital input–output interface (NI-9375).
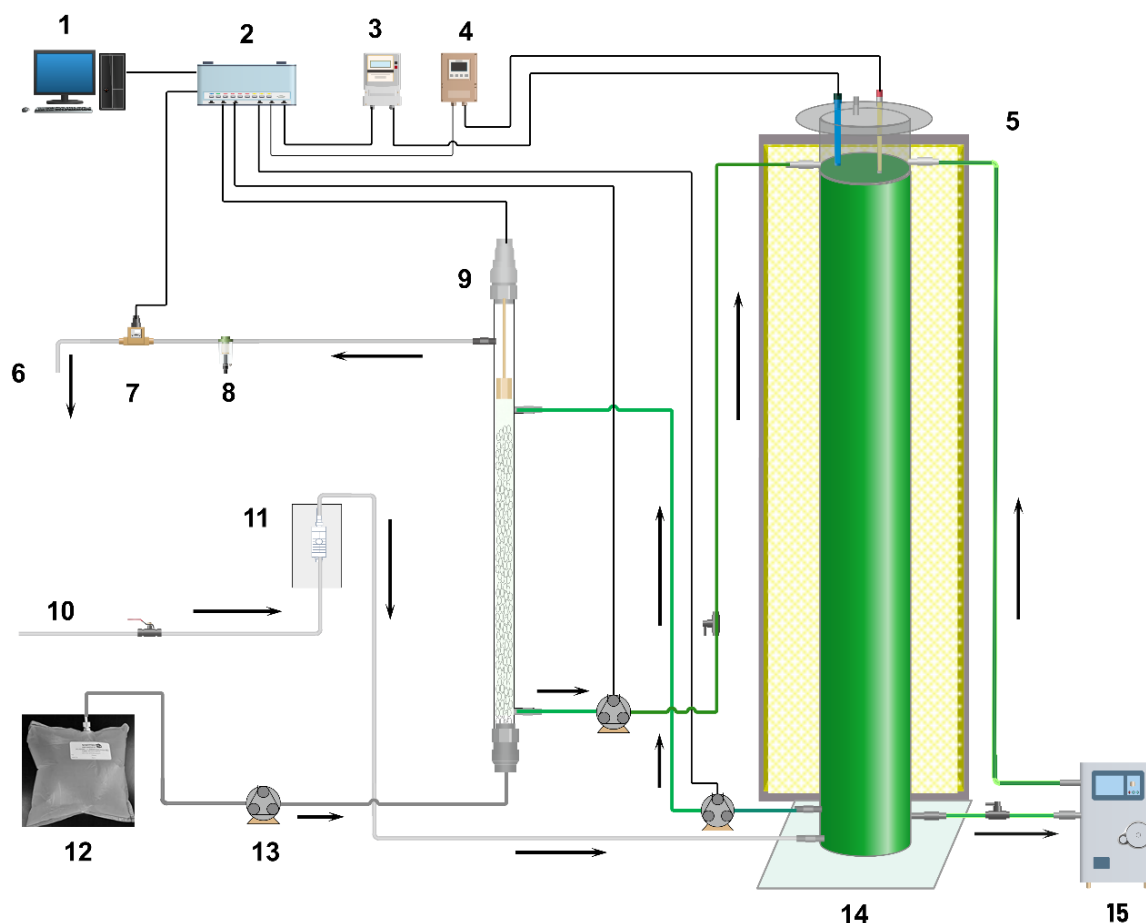

Figure 1. Schematic diagram of the two-stage system that includes the absorption column and the photobioreactor. **1.** Computer, **2.** cDAQ Chassis, **3.** dissolved oxygen sensor/transmitter, **4.** pH sensor/transmitter, **5.** led panels, **6.** biogas substitute outlet, **7.** CO_2 sensor/transmitter, **8.** filter, **9.** CO_2 absorption column, **10.** air inlet, **11.** flow meter, **12.** biogas substitute, **13.** peristaltic pump, **14.** photobioreactor, **15.** thermostatic bath.

2.2. Experimental Conditions

Two nutrient solutions were used: COMBO medium [26] enriched in phosphorus (5 mM) and nitrogen (5 mM NaNO$_3$), and landfill leachate. The COMBO medium was fed semi-continuously, with between 2 and 5 L of culture being removed in order to maintain the biomass concentration at between 1.2 and 1.4 g TSS L^{-1}. The nitrate concentration was

between 15 and 30 mg N-NO$_3^-$ L^{-1}. The landfill leachate composition is summarized in Table 1. The non-axenic microalgae consortium was isolated [27] from landfill leachate obtained from the "Miramundo-Los Hardales" landfill (Cadiz, Spain), location: 36°28′42.5″ N, 6°00′56.1″ W. The microalgae were spherical and had a homogenous size (3.67 ± 0.6 μm) (Figure S1), with a total protein content of 39.5%, and was able to store lipids under nitrogen and phosphorus limitation up to 53% after 9 d with COMBO medium (2 mM NaNO3) [27]. The predominant species based on size and protein and lipid concentration could belong to *Nannochloropsis* sp. or *Chlorella* sp. [27].

Table 1. Composition of landfill leachate.

Parameter	Value	Unit
pH	7.86 ± 0.01	-
Conductivity	41.4 ± 0.46	mS cm^{-1}
Chemical oxygen demand (COD)	8991 ± 227	mg O$_2$ L^{-1}
Alkalinity	17,977 ± 244	mg CaCO$_3$ L^{-1}
Total suspended solids (TSS)	17,418 ± 137	mg L^{-1}
Total volatile solids (TVS)	6297 ± 61	mg L^{-1}
Total phosphorous	82.77 ± 0.77	mg L^{-1}
P-PO$_4^{3-}$	43.99 ± 1.20	mg L^{-1}
Total nitrogen	4613 ± 93	mg L^{-1}
N-NH$_4^+$	3785 ± 174	mg L^{-1}
N-NO$_3^-$	n.d.	mg L^{-1}
N-NO$_2^-$	n.d.	mg L^{-1}
S-SO$_4^{2-}$	92.72 ± 0.57	mg L^{-1}
Cl$^-$	5939 ± 172	mg L^{-1}
Br$^-$	24.01 ± 2.83	mg L^{-1}
Na	3920 ± 12	mg L^{-1}
K	1957 ± 22	mg L^{-1}
Ca	42.1 ± 0.6	mg L^{-1}
Mg	49.0 ± 1.3	mg L^{-1}
Si	<40 *	mg L^{-1}
Sr	3.34 ± 0.10	mg L^{-1}
V	<0.200 *	mg L^{-1}
Mn	0.160 ± 0.010	mg L^{-1}
Fe	8.10 ± 0.10	mg L^{-1}
Co	0.075 ± 0.002	mg L^{-1}
Cu	0.102 ± 0.001	mg L^{-1}
Zn	0.970 ± 0.170	mg L^{-1}
Se	<0.240 *	mg L^{-1}
Hg	<0.030 *	mg L^{-1}
Pb	0.020 ± 0.002	mg L^{-1}

n.d. = non detected. * Below detection limit.

The experimental conditions are summarized in Table 2, and each experimental condition was performed in duplicate. Experiment 1 allowed us to establish what flow mode (co-current or counter-current) was most suitable for the maximum removal of CO$_2$. Three L/G ratios were used at an inlet CO$_2$ concentration of 40%. In experiment 2, the effect of L/G ratio on the CO$_2$ and O$_2$ outlet biogas concentrations was analyzed. The absorption column flow mode was counter-current and L/G was 1, 1.5, 2 and 4. The inlet CO$_2$ concentration was 20% and 40%. In experiment 3, landfill leachate was used as a nutrient source, with the L/G ratio being fixed at 1.5 and an inlet CO$_2$ concentration of 20% and 40%. The photobioreactor was adapted to leachate gradually over 18 days. Initially, 3 L of the liquid medium was removed and replaced with diluted leachate, reaching an approximate concentration of 1 mM N-NH$_4^+$. Additional periodic replacements were performed when the N-NH$_4^+$ concentration dropped below 0.4 mM.

Table 2. Summary of the experimental conditions.

Experimental Conditions	Nutrient Solution	Flow Mode	L/G	Inlet CO_2 Concentration
1	COMBO	co-current or counter-current	1, 2, 4	40%
2	COMBO	counter-current	1, 1.5, 2, 4	20%, 40%
3	Leachate	counter-current	1.5	20%, 40%
4	Leachate	counter-current	1.5	20%

Experiment 3 considers the combined use of leachate and nitrifying bacteria. The inlet CO_2 concentration and L/G were 20% and 1.5, respectively. Leachate was fed into the photobioreactor to obtain a maximum nitrogen concentration of 2 mM $N\text{-}NH_4^+$. In experiment 4, a nitrifying bacterial culture was used. This culture was obtained from a laboratory continuous stirred tank bioreactor (CSTBR) operated for 354 days with a synthetic eluent (ammonium-rich water) [28].Two inoculation procedures were carried out:

- Inoculation of the photobioreactor: 2 L of nitrifying bacterial culture were added directly to the photobioreactor. To avoid light inhibition of the nitrifying bacteria, the lower third of the bubble column was covered.
- Inoculation of the absorption column: the absorption column recirculated the nitrifying culture for 15 days, thus allowing biofilm formation on the Rasching rings.

2.3. Analytical Methods

The inlet CO_2 concentration was measured by gas chromatography (GC-450, BRUKER, Berlin, Germany) with a Thermal Conductivity Detector and Poraplot Q plot FS 25 m $\times$ 0.53 mm column. The outlet CO_2 concentration was measured using an infrared CO_2 transmitter (2112BC4-V, Euro-Gas, Devon, UK). Total suspended solids (TSS) was determined according to Standard Method 2540-C [29]. Nitrate and ammonium concentrations were determined by ion chromatography (Metrohm 930 Compact IC Flex, Herisau, Switzerland).

2.4. Fitting to Empirical Model

The experimental results were fitted with an empirical model. A second-order polynomial model was used to predict the outlet CO_2 concentration as the response variable. The independent variables were the L/G ratio and the inlet CO_2 concentration. The levels of the L/G ratio were 1, 1.5, 2 and 4 and the levels for the inlet CO_2 concentration were 20% and 40%. The data were analyzed using Statgraphics® Centurion 19 (v.19.1.3)

3. Results and Discussion

3.1. Optimization of the Two-Stage System

The photobioreactor was first operated with the COMBO synthetic medium for 55 days. Figure 2 shows the evolution of biomass and nitrogen concentration in the form of nitrate. The nitrate concentration was 24.95 $\pm$ 3.41 mg $N\text{-}NO_3^-$ L^{-1}, the DO was 9.69 $\pm$ 0.14 mg O_2 L^{-1} and pH was 8.7 $\pm$ 0.1. Under these operating conditions, the average biomass concentration and biomass productivity were 1.28 $\pm$ 0.05 g TSS L^{-1} and 31.0 $\pm$ 11.7 g m^{-3} d^{-1}, respectively. Other authors have reported similar productivities. For example, Chiu et al. [30] described a semi-continuous operation with *Nannochloropsisoculata* and obtained a productivity of between 37 and 48 g m^{-3} d^{-1}, and a biomass concentration of between 0.75 and 0.92 g TSS L^{-1} for a CO_2 concentration in the range 2–15%. In another example, Ruiz et al. [31] obtained a productivity of 17 g m^{-3} d^{-1} with a culture of *Chlorella vulgaris*.
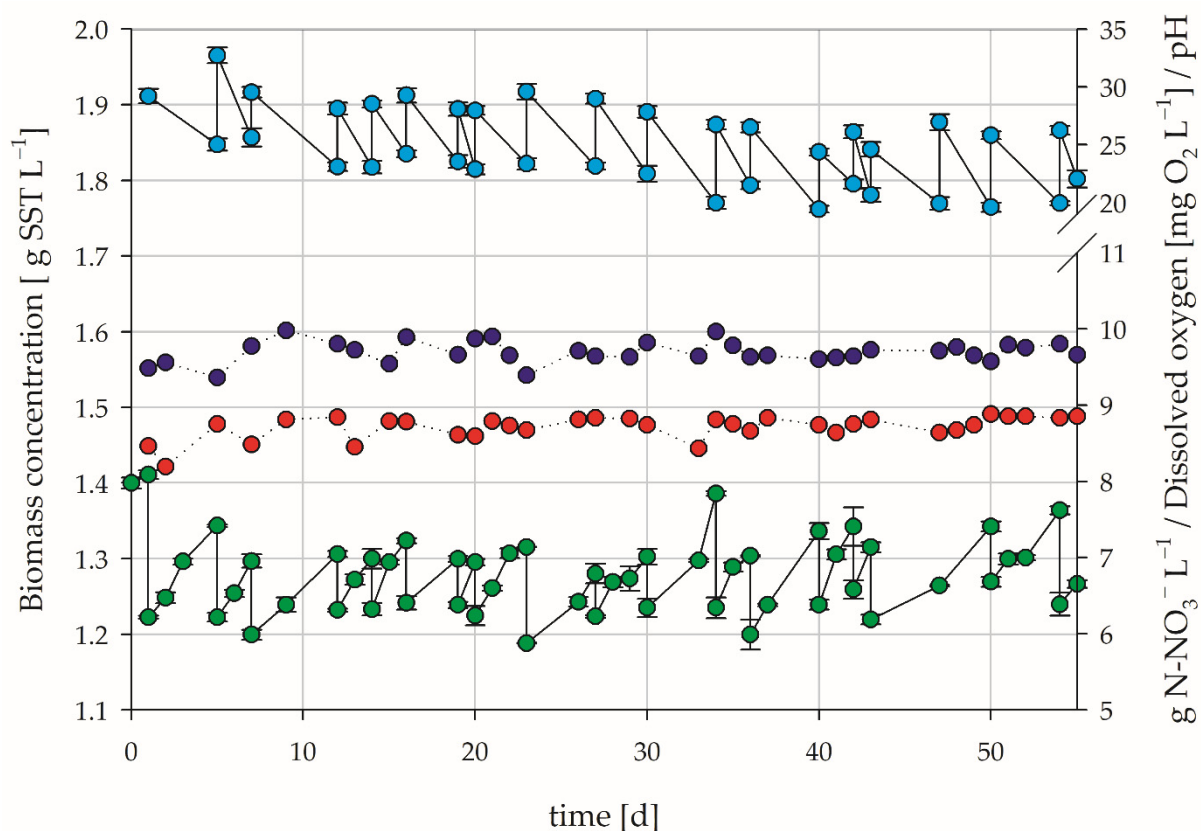
Figure 2. Photobioreactor behavior under steady-state operation using COMBO medium. pH (red) and biomass (green), nitrate (light blue), and DO (dark blue) concentrations.

The pH is of great importance in the absorption of acidic gases such as CO_2. Thus, the gas–liquid equilibrium changes as a function of pH, and this change in equilibrium can be described by a coefficient relating Henry's law constant, dissociation constants, and pH [25] (Figure S2). This coefficient relates the concentration in the gas and in the liquid at equilibrium. For example, at a pH of 8.5, the value is $7 \cdot 10^{-3}$, while for pH 9.5, it is $6.2 \cdot 10^{-4}$, thus indicating that an increase of 1 pH point causes the gas to be 11 times more soluble.

3.1.1. Effect of Flow Mode in the Absorption Column

Figure 3a shows the concentration of CO_2 and O_2 at the outlet stream of the absorption column for the three L/G ratios studied (1, 2 and 4), for both counter-current and co-current flow. The stabilization period for CO_2 and O_2 outlet concentrations was between 4 and 6 h (example in Figure 3b). A statistically significant difference (Multifactor ANOVA, L/G p-value < 0.0001 and flow mode p-value = 0.0020) between CO_2 concentration and both factors was found. It can be seen how an increase in L/G causes a greater absorption of CO_2 and, therefore, a lower concentration in the output gas stream. On the other hand, an increase in L/G also causes a greater O_2 desorption and, therefore, an increase in the outlet O_2 concentration. Figure 3a also shows that CO_2 absorption was higher when the flow was in counter-current, with an outlet concentration of 0.4% being obtained when L/G was 2, compared to the value of 10.9% in the co-current experiment. In contrast, O_2 desorption was slightly lower when the flows were co-current. For an L/G of 4, the values were 2.1% and 2.5% for co-current and counter-current flows, respectively. In view of these results, a counter-current flow and an L/G ratio of 2 resulted in the lowest outlet concentration in the absorption column, giving a combined CO_2 and O_2 concentration of 2.2%. The average DO concentrations in the photobioreactor were 9.60 ± 0.03 and 9.70 ± 0.04 mg O_2 L^{-1} for the co-current and counter-current experiments, respectively.
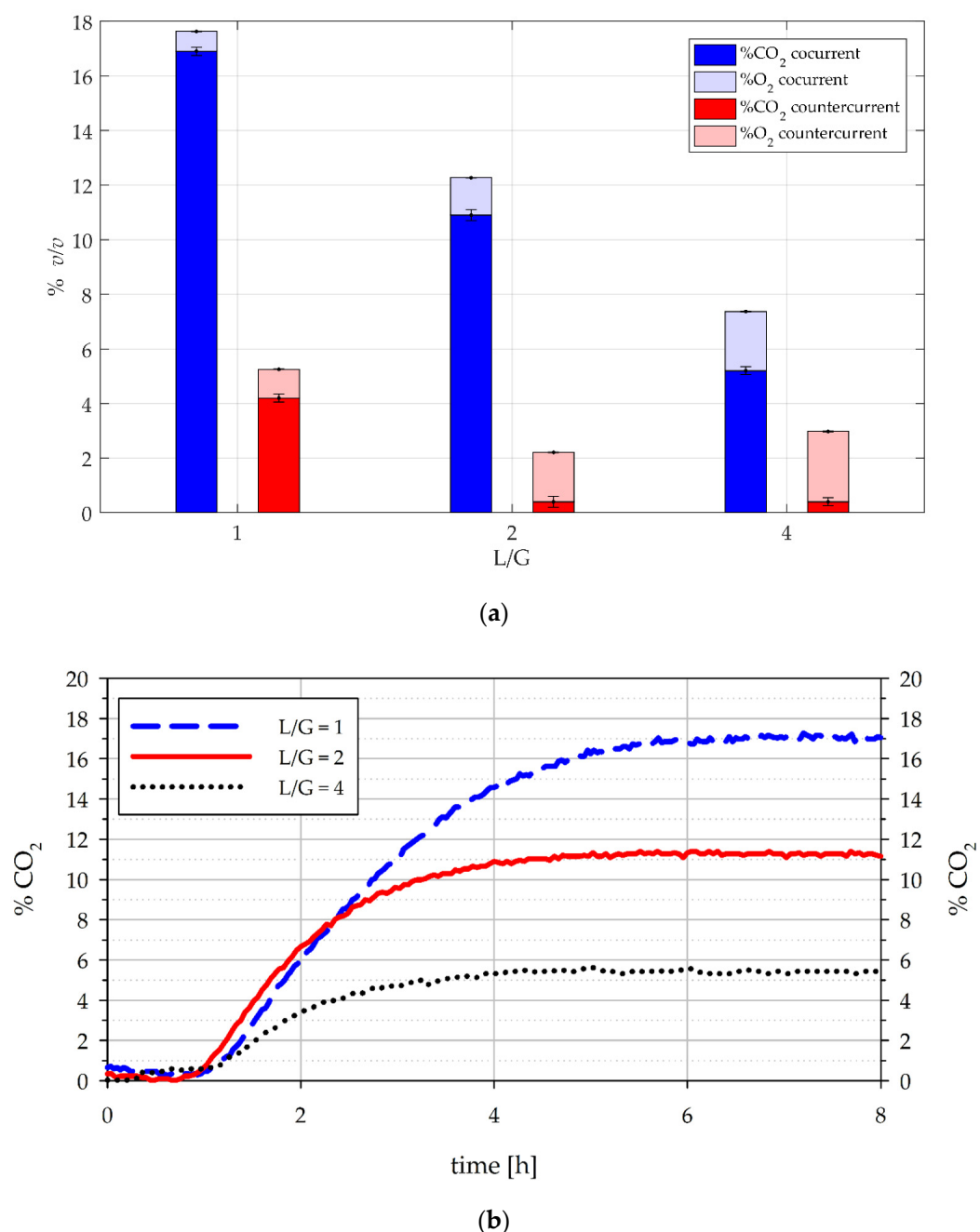
(a)

(b)

Figure 3. (**a**) Absorption column outlet CO_2 and O_2 concentrations in co-current and counter-current flow modes for an L/G of 1, 2 and 4. (**b**) Outlet CO_2 concentration at the absorption column operating in co-current.

Most of the literature reports use an absorption column in co-current mode. Toledo-Cervantes et al. [8], for example, evaluated the effect of gas–liquid flow configuration on absorption column performance in a co-current configuration and obtained a biomass productivity of 15 g m^{-2} d^{-1}, whereas biomass productivity decreased to 8.7 $\pm$ 0.5 g m^{-2} d^{-1} in counter-current due to a limitation of trace metals. This limitation was caused by the precipitation of metal sulfides due to the low DO concentration in the lower part of the absorption column, where the liquid stream is brought into contact with biogas with a higher concentration of hydrogen sulfide. These authors observed a lower CO_2 concentration when the operation was co-current, whereas O_2 and N_2 concentrations did not differ significantly. The best configuration was obtained at an L/G ratio of 0.5 and co-current operation. Similarly, Serejo et al. [32] obtained a CO_2 removal efficiency of 80%, and less

than 2% O_2, using an L/G ratio of 10 in co-current mode together with synthetic biogas with a CO_2 concentration of 30%. Toledo-Cervantes et al. [33] obtained a removal efficiency of 98.6% using an absorption column fed with alga-bacterial broth at a pH of 10 ± 0.3. These authors also observed that part of the O_2 and N_2 is desorbed on the absorption column in proportion to the L/G ratio. For an L/G of 5, Franco-Mortado et al. [34] found an outlet CO_2 concentration of between 1.8% and 3.3% and an outlet O_2 concentration of 2.6% in a system operating at pH 9.5, and Rodero et al. [35] used a counter-current configuration in a semi-industrial scale system. The maximum biomethane concentration of 90% was limited by desorption of N_2 and O_2. Finally, Marin et al. [36] used an absorption unit in which gas and liquid flows were co-current (L/G ratio of 0.5). These authors used various operating strategies: with no aeration of the photobioreactor, the CO_2 concentration of purified biogas was up to 6.1% and the pH was 9.1, whereas with aeration (1 vvm), they obtained a biogas CO_2 concentration of 0.3–0.4% and pH of 9.8.

3.1.2. Influence of L/G and Inlet Concentration

The L/G ratio mainly affects two aspects of CO_2 absorption, namely the superficial liquid velocity, which can affect the mass-transfer coefficient, and the concentration of inorganic carbon along the absorption column. Thus, at a liquid velocity of between 0.001 and 0.005 m s^{-1}, the mass transfer coefficients were similar to that obtained for a flow rate equal to 0 (3.46 ± 0.05 h^{-1}). When operating at a higher ratio, the inorganic carbon concentration will be lower, thus causing a higher driving force for the absorption of CO_2 contained in the biogas. This phenomenon can be seen in Figure 4. Statistical analysis shows dependence between CO_2 concentration and L/G ration and inlet CO_2 concentration (Multifactor ANOVA, L/G p-value =0.0042 and inlet CO_2 p-value = 0.0082). For instance, when the L/G ratio was increased from 1 to 4, the outlet CO_2 concentration decreased from 1.5% to 0.1% (inlet CO_2 of 20%), or from 4.2% to 0.4% (inlet CO_2 of 40%). It is interesting to note that an increase in L/G ratio from 2 to 4 did not result in an increase in CO_2 uptake. The specific CO_2 removal rate ranged between 0.25 and 0.27 g L^{-1} h^{-1} for 20% CO_2 and between 0.51 and 0.54 g L^{-1} h^{-1} at a value of 40%.
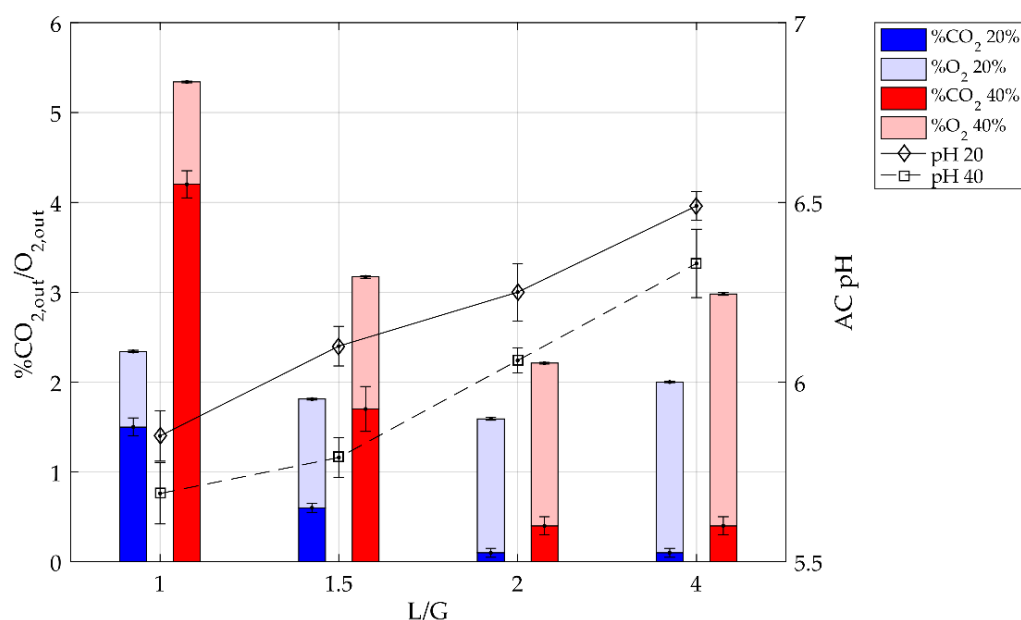

Figure 4. Absorption column outlet CO_2 and O_2 concentration and outlet pH for L/G of 1, 1.5, 2 and 4 and inlet CO_2 concentrations of 20% and 40%.

The pH in the absorption column depends on the quantity of CO_2 absorbed, the liquid flow rate and the concentration of inorganic carbon in the liquid stream from the photobioreactor. At a CO_2 concentration of 20%, the pH in the photobioreactor remained

constant at 8.3. In contrast, at a CO_2 concentration of 40%, the pH at the end of the experiments varied as a function of the liquid flow rate, decreasing from a value of 8.05 when the L/G ratio was 1 to a value of 7.79 when the L/G ratio was 4. With regard to the pH in the absorption column at the end of each experiment, as can be seen in Figure 4, this value was proportional to the L/G ratio, and an increase in the inlet CO_2 concentration caused a decrease in pH. Indeed, a lower decrease in pH between the inlet and outlet of the absorption column was observed with increasing L/G ratio (ΔpH of 2.45, 2.2, 2.06 and 1.79 for 20% CO_2 and a ΔpH of 2.36, 2.22, 1.82 and 1.46 for 40% CO_2). In this regard, Rodero et al. [35] observed that the highest CO_2 uptake occurred at the highest L/G ratio evaluated (3.5). The absorption column inlet CO_2 concentration in that study was 32.7 ± 2.8%, and a removal efficiency of 88.9 ± 1.5% was obtained at a biogas flow rate of 274 L h^{-1}. These authors also observed a pH decrease of 1.7, 1.5 and 1.2 for L/G ratios of 1.2, 2.1 and 3.5, respectively. The removal efficiency obtained in this study, for similar operating conditions (40% CO_2 and L/G equal to 4) was 99.39%. Marin et al. [37] found that the maximum CO_2 absorption was obtained for an L/G ratio of two, with removal efficiencies in the range 90.4–99.9%. These authors also found that the concentration of N_2 and O_2 increased from 3.4% for an L/G ratio of 0.5 to 11.9% at a ratio of five due to desorption processes.

3.1.3. Empirical Model

The statistical results show the significance and high predictability of the regression model. The R-squared was 86.64%, the residual standard deviation was 0.5990, and the mean absolute error was 0.4166. The second-order polynomial model fitted with calibration data is represented by Equation (1).

$$\% \ CO_{2\ out} = 2.15527 - 3.4844{\cdot}L/G + 0.139575{\cdot}CO_{2\ in} + 0.762422{\cdot}(L/G)^2 - 0.036506{\cdot}L/G{\cdot}CO_{2\ in} \tag{1}$$

The most influential factor on the outlet CO_2 concentration was the L/G (Figure S3) with a negative effect. The model can be used to predict the optimum L/G ratio to achieve the minimum outlet CO_2 concentration for the specified inlet CO_2. Therefore, for an inlet concentration of 20%, the optimum L/G would be 2.76, for an inlet concentration of 30%, the L/G ratio would be 3.00 and for 40%, the L/G would be 3.24

3.2. Use of Leachate as Culture Medium

Leachate was used as culture medium for 20 days. As can be seen in Figure 5, the biomass concentration remained in the same range: 1.51 ± 0.08 g TSS L^{-1} when the photobioreactor was operated with COMBO medium, and 1.52 ± 0.09 g TSS L^{-1} when operated with leachate. DO was maintained at 8.88 ± 0.20 mg O_2 L^{-1}, whereas the pH decreased from 8.2 ± 0.2 to 6.9 ± 0.1. In order to use pH conditions similar to those used with COMBO medium, the pH was increased prior to the absorption column experiments.

The L/G used (1.5) was lower than the optimum found in order to observe any possible improvement in the removal efficiency of the absorption column. Figure 6 shows the outlet concentrations of CO_2 and O_2 and the outlet pH of the absorption column. When COMBO medium was used, the CO_2 concentration at the outlet was 0.6% and 1.7% for inlet concentrations of 20% and 40%, respectively. The DO concentrations in the photobioreactor were 9.79 and 9.65 mg O_2 L^{-1}, and the estimated O_2 concentration in the output gas was 1.21% and 1.47%, respectively. On the other hand, when leachate was used as the culture medium, the concentrations at the outlet were 0.01% and 0.6% for CO_2 and 1.09% and 1.37% for O_2 for inlet CO_2 concentrations of 20% and 40%, respectively. A lower DO of 8.81 and 8.89 mg O_2 L^{-1}, respectively, was measured when leachate was used. Multifactorial ANOVA analysis showed a correlation between the outlet CO_2 and nutrient solution and inlet CO_2 with a p-value equal to 0.0406 for the nutrient solution and 0.0390 for inlet CO_2.
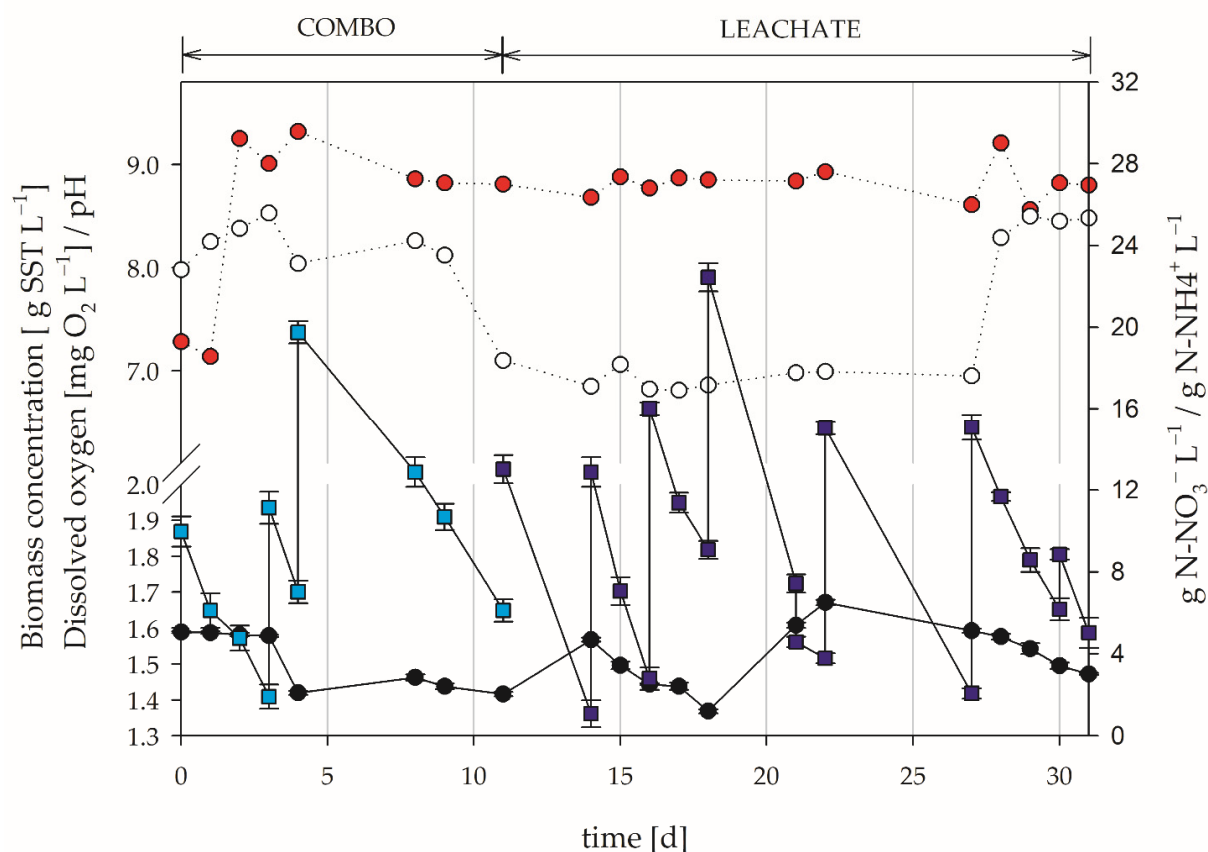
Figure 5. Photobioreactor behavior in steady-state operation using landfill leachate as medium. Concentration of biomass (black circle), nitrate (light blue square), ammonium (blue square), DO (red circle) and pH (white circle).
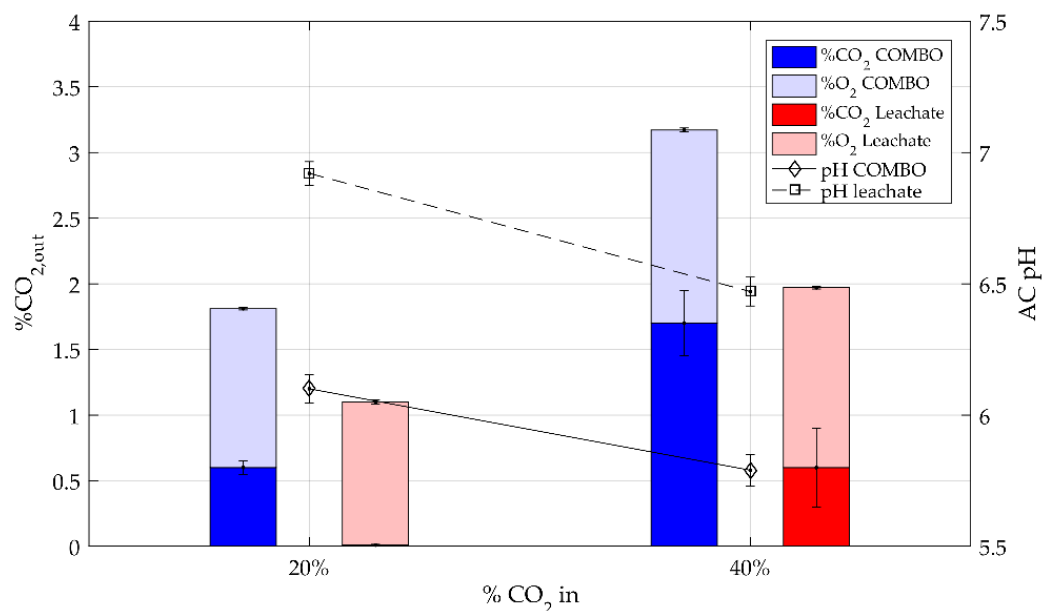

Figure 6. Absorption column outlet CO_2 and O_2 concentrations and outlet pH for *L/G* 1.5 and inlet CO_2 concentrations of 20% and 40% for nutrient solution COMBO and landfill leachate.

A smaller pH drop in the absorption column was observed when leachate was used (ΔpH of 2.20 vs. 1.34 for 20% CO_2 and ΔpH of 2.22 vs. 1.54 for 40% CO_2). This resulted in a higher pH at the outlet of the absorption column when leachate was used, as can be seen in Figure 6, and thus higher CO_2 solubility and better absorption overall. This

behavior is due to the higher alkalinity found in the culture medium from leachate. The beneficial influence of alkalinity on CO_2 removal has been reported by various authors. For example, Marin et al. [37] found that an increase in alkalinity resulted in a higher CO_2 removal capacity, and these authors found a clear decrease in the absorption column output concentration with an increase in alkalinity from 42 ± 1 to 1557 ± 26 mg L^{-1} associated with the increase in pH of the culture medium (from 6.5 ± 0.1 to 9.3 ± 0.0).

3.3. Inoculation with Nitrifying Bacteria

Two strategies were employed. The first strategy allowed the formation of a biofilm of nitrifying bacteria on the support material of the absorption column by recirculating a suspension culture from a CSTBR, whereas in the second strategy, 2 L of culture medium with nitrifying bacteria was added directly to the photobioreactor, one-third of which was covered to provide darkness. The pH in the photobioreactor was 7.54. Both nitrosation [38] and NH_4^+ consumption by the microalgae release protons into the medium, thus contributing to its acidification, whereas NO_3^- assimilation causes a slight increase in pH [39]. The inoculation period for the nitrifying bacterial consortium in the rings lasted 15 days. Once this time had elapsed, the absorption column was placed in contact with the photobioreactor and bacterial aggregates were found to form, thus indicating possible detachment of the bacteria that formed the biofilm in the Rasching rings. The presence of nitrifying bacteria decreased the O_2 concentration in the photobioreactor from 8.81 to 8.22 and 8.17 mg O_2 L^{-1} when attached to the support and in suspension, respectively. The consumption of ammonium by the bacteria to generate nitrate decreases the pH, whereas the consumption of nitrate by the microalgae consumes protons. The pH in the photobioreactor was 7.54, lower than that found without bacteria under similar conditions (8.26). The decrease in pH caused less-efficient CO_2 absorption, with a CO_2 concentration at the outlet of the absorption column of 1%.

The presence of NH_4^+ in the culture medium inhibits the consumption of nitrate by the microalgae [27]. During the experimental period, the ammonium concentration decreased from 30.5 to 3.0 mg N-NH_4^+ L^{-1} and the final nitrate concentration was 19.7 mg N-NO_3^- L^{-1}. Saldarriaga et al. [27] reported an ammonium inhibition constant for specific nitrate uptake of 0.75 mg NH_4^+ L^{-1}, at a concentration of 3.0 mg NH_4^+ L^{-1}, thus meaning that the specific rate of nitrite uptake is inhibited by 80%. This fact explains the competitive consumption of ammonium by nitrifying bacteria and microalgae and the accumulation of nitrate in the culture medium. It is therefore necessary to look for an alternative strategy to consume the O_2 produced in the photobioreactor, preferably involving the combined and symbiotic action of microorganisms. These strategies may concern the use of the oxygen content in biogas as an electron acceptor. An example could be the use of an aerobic desulphurization unit, adding sulfur or thiosulphate as the electron donor; a possible handicap is the production of hydrogen sulfide in reductive ambient. Low oxygen concentration and solubility will require the use of gas transfer enhancements, as can be the use of oxygen vectors, such as n-dodecane.

4. Conclusions

The use of a two-stage system comprising an absorption column and a photobioreactor has been successfully implemented. Landfill leachate has been found to be a feasible nutrient source, and it has also been demonstrated that the CO_2 contained in the biogas can be more efficiently removed. In addition, the O_2 concentration in the biogas leaving the absorber was lower. When leachate was used, the pH of the photobioreactor was similar to that recorded when COMBO medium was used, whereas the pH in the absorber was 0.77 ± 0.12 higher. As such, we can conclude that the greater buffer capacity of the medium containing landfill leachate allows operation under conditions in which the solubility of CO_2 was higher. A reduction in DO in the photobioreactor of 0.87 ± 0.15 mg O_2L^{-1} was also observed.

The inoculation of nitrifying bacteria had two effects. Firstly, the DO decreased in the whole system, therefore the outlet O_2 concentration was lower, and secondly, there was simultaneous consumption of NH_4^+ by both the nitrifying bacteria and the microalgae, thus favoring an acidification of the medium. A higher outlet CO_2 concentration was observed as a result of the lower pH than that found before the inoculation of bacteria.

References

1. European Commission. Communication from the Commission to the European Parliament, the European Council, the Council, the European Economic and Social Committee, the Committee of the Regions and the European Investment Bank a Clean Planet for All a European Strategic Long-Term. Available online: https://eur-lex.europa.eu/legal-content/EN/TXT/?uri=CELEX:52018DC0773 (accessed on 16 November 2020).
2. European Commission. Communication from the Commission to the European Parliament, the Council, the European Economic and Social Committee and the Committee of the Regions a Roadmap for Moving to a Competitive Low Carbon Economy in 2050. Available online: https://eur-lex.europa.eu/legal-content/EN/ALL/?uri=CELEX:52011DC0112 (accessed on 21 June 2021).
3. Sun, Q.; Li, H.; Yan, J.; Liu, L.; Yu, Z.; Yu, X. Selection of appropriate biogas upgrading technology-a review of biogas cleaning, upgrading and utilisation. *Renew. Sustain. Energy Rev.* **2015**, *51*, 521–532. [CrossRef]
4. Baena-Moreno, F.M.; Rodríguez-Galán, M.; Vega, F.; Vilches, L.F.; Navarrete, B. Review: Recent advances in biogas purifying technologies. *Int. J. Green Energy* **2019**, *16*, 401–412. [CrossRef]
5. Ouyang, Y.; Zhao, Y.; Sun, S.; Hu, C.; Ping, L. Effect of light intensity on the capability of different microalgae species for simultaneous biogas upgrading and biogas slurry nutrient reduction. *Int. Biodeterior. Biodegrad.* **2015**, *104*, 157–163. [CrossRef]
6. Srinuanpan, S.; Cheirsilp, B.; Prasertsan, P. Effective biogas upgrading and production of biodiesel feedstocks by strategic cultivation of oleaginous microalgae. *Energy* **2018**, *148*, 766–774. [CrossRef]
7. Bahr, M.; Díaz, I.; Dominguez, A.; González Sánchez, A.; Muñoz, R. Microalgal-Biotechnology as a platform for an integral biogas upgrading and nutrient removal from anaerobic effluents. *Environ. Sci. Technol.* **2014**, *48*, 573–581. [CrossRef] [PubMed]
8. Toledo-Cervantes, A.; Madrid-Chirinos, C.; Cantera, S.; Lebrero, R.; Muñoz, R. Influence of the gas-liquid flow configuration in the absorption column on photosynthetic biogas upgrading in algal-bacterial photobioreactors. *Bioresour. Technol.* **2017**, *225*, 336–342. [CrossRef] [PubMed]
9. Toledo-Cervantes, A.; Morales, T.; González, Á.; Muñoz, R.; Lebrero, R. Long-term photosynthetic CO_2 removal from biogas and flue-gas: Exploring the potential of closed photobioreactors for high-value biomass production. *Sci. Total Environ.* **2018**, *640–641*, 1272–1278. [CrossRef] [PubMed]
10. Meier, L.; Pérez, R.; Azócar, L.; Rivas, M.; Jeison, D. Photosynthetic CO_2 uptake by microalgae: An attractive tool for biogas upgrading. *Biomass Bioenergy* **2015**, *73*, 102–109. [CrossRef]
11. Prandini, J.M.; da Silva, M.L.B.; Mezzari, M.P.; Pirolli, M.; Michelon, W.; Soares, H.M. Enhancement of nutrient removal from swine wastewater digestate coupled to biogas purification by microalgae *Scenedesmus* spp. *Bioresour. Technol.* **2016**, *202*, 67–75. [CrossRef] [PubMed]
12. Bilanovic, D.; Holland, M.; Starosvetsky, J.; Armon, R. Co-cultivation of microalgae and nitrifiers for higher biomass production and better carbon capture. *Bioresour. Technol.* **2016**, *220*, 282–288. [CrossRef]
13. Mairet, F.; Ramírez, C.H.; Rojas-Palma, A. Modeling and stability analysis of a microalgal pond with nitrification. *Appl. Math. Model.* **2017**, *51*, 448–468. [CrossRef]

14. Rada-Ariza, A.M.; Lopez-Vazquez, C.M.; van der Steen, N.P.; Lens, P.N.L. Nitrification by microalgal-bacterial consortia for ammonium removal in flat panel sequencing batch photo-bioreactors. *Bioresour. Technol.* **2017**, *245*, 81–89. [CrossRef] [PubMed]

15. Choi, O.; Das, A.; Yu, C.-P.; Hu, Z. Nitrifying bacterial growth inhibition in the presence of algae and cyanobacteria. *Biotechnol. Bioeng.* **2010**, *107*, 1004–1011. [CrossRef]

16. Noorain, R.; Kindaichi, T.; Ozaki, N.; Aoi, Y.; Ohashi, A. Biogas purification performance of new water scrubber packed with sponge carriers. *J. Clean. Prod.* **2019**, *214*, 103–111. [CrossRef]

17. Läntelä, J.; Rasi, S.; Lehtinen, J.; Rintala, J. Landfill gas upgrading with pilot-scale water scrubber: Performance assessment with absorption water recycling. *Appl. Energy* **2012**, *92*, 307–314. [CrossRef]

18. Tan, L.S.; Shariff, A.M.; Lau, K.K.; Bustam, M.A. Factors affecting CO_2 absorption efficiency in packed column: A review. *J. Ind. Eng. Chem.* **2012**, *18*, 1874–1883. [CrossRef]

19. Sunda, W.G.; Price, N.M.; Morel, F.M.M. Trace metal ion buffers and their use in culture studies. In *Algal Culturing Techniques*; Elsevier: Amsterdam, The Netherlands, 2005; pp. 35–63.

20. Markou, G.; Nerantzis, E. Microalgae for high-value compounds and biofuels production: A review with focus on cultivation under stress conditions. *Biotechnol. Adv.* **2013**, *31*, 1532–1542. [CrossRef]

21. Cuellar-Bermudez, S.P.; Aleman-Nava, G.S.; Chandra, R.; Garcia-Perez, J.S.; Contreras-Angulo, J.R.; Markou, G.; Muylaert, K.; Rittmann, B.E.; Parra-Saldivar, R. Nutrients utilization and contaminants removal. A review of two approaches of algae and cyanobacteria in wastewater. *Algal Res.* **2017**, *24*, 438–449. [CrossRef]

22. Park, K.C.; Whitney, C.G.E.; Kozera, C.; O'Leary, S.J.B.; McGinn, P.J. Seasonal isolation of microalgae from municipal wastewater for remediation and biofuel applications. *J. Appl. Microbiol.* **2015**, *119*, 76–87. [CrossRef]

23. Khanzada, Z.T.; Övez, S. Microalgae as a sustainable biological system for improving leachate quality. *Energy* **2017**, *140*, 757–765. [CrossRef]

24. Nordin, N.; Yusof, N.; Samsudin, S. Biomass Production of *Chlorella* sp., *Scenedesmus* sp., and *Oscillatoria* sp. in nitrified landfill leachate. *Waste Biomass Valorization* **2017**, *8*, 2301–2311. [CrossRef]

25. Zhao, X.; Zhou, Y.; Huang, S.; Qiu, D.; Schideman, L.; Chai, X.; Zhao, Y. Characterization of microalgae-bacteria consortium cultured in landfill leachate for carbon fixation and lipid production. *Bioresour. Technol.* **2014**, *156*, 322–328. [CrossRef] [PubMed]

26. Kilham, S.S.; Kreeger, D.A.; Lynn, S.G.; Goulden, C.E.; Herrera, L. COMBO: A defined freshwater culture medium for algae and zooplankton. *Hydrobiologia* **1998**, *377*, 147–159. [CrossRef]

27. Saldarriaga, L.F.; Almenglo, F.; Ramírez, M.; Cantero, D. Kinetic characterization and modeling of a microalgae consortium isolated from landfill leachate under a high CO_2 concentration in a bubble column photobioreactor. *Electron. J. Biotechnol.* **2020**, *44*, 47–57. [CrossRef]

28. González-Cortés, J.J.; Almenglo, F.; Ramírez, M.; Cantero, D. Simultaneous removal of ammonium from landfill leachate and hydrogen sulfide from biogas using a novel two-stage oxic-anoxic system. *Sci. Total Environ.* **2021**, *750*, 141664. [CrossRef] [PubMed]

29. APHA. *Standard Methods for the Examination of Water and Wastewater*, 22nd ed.; Rice, E.W., Baird, R.B., Eaton, A.D., Clesceri, L.S., Eds.; American Public Health Association: Washington, DC, USA, 2012.

30. Chiu, S.-Y.; Kao, C.-Y.; Tsai, M.-T.; Ong, S.-C.; Chen, C.-H.; Lin, C.-S. Lipid accumulation and CO_2 utilization of Nannochloropsis oculata in response to CO_2 aeration. *Bioresour. Technol.* **2009**, *100*, 833–838. [CrossRef] [PubMed]

31. Ruiz, J.; Arbib, Z.; Álvarez-Díaz, P.D.; Garrido-Pérez, C.; Barragán, J.; Perales, J.A. Photobiotreatment model (PhBT): A kinetic model for microalgae biomass growth and nutrient removal in wastewater. *Environ. Technol.* **2013**, *34*, 979–991. [CrossRef]

32. Serejo, M.L.; Posadas, E.; Boncz, M.A.; Blanco, S.; García-Encina, P.; Muñoz, R. Influence of biogas flow rate on biomass composition during the optimization of biogas upgrading in microalgal-bacterial processes. *Environ. Sci. Technol.* **2015**, *49*, 3228–3236. [CrossRef]

33. Toledo-Cervantes, A.; Serejo, M.L.; Blanco, S.; Pérez, R.; Lebrero, R.; Muñoz, R. Photosynthetic biogas upgrading to bio-methane: Boosting nutrient recovery via biomass productivity control. *Algal Res.* **2016**, *17*, 46–52. [CrossRef]

34. Franco-Morgado, M.; Alcántara, C.; Noyola, A.; Muñoz, R.; González-Sánchez, A. A study of photosynthetic biogas upgrading based on a high rate algal pond under alkaline conditions: Influence of the illumination regime. *Sci. Total Environ.* **2017**, *592*, 419–425. [CrossRef]

35. del Rosario Rodero, M.; Lebrero, R.; Serrano, E.; Lara, E.; Arbib, Z.; García-Encina, P.A.; Muñoz, R. Technology validation of photosynthetic biogas upgrading in a semi-industrial scale algal-bacterial photobioreactor. *Bioresour. Technol.* **2019**, *279*, 43–49. [CrossRef]

36. Marín, D.; Carmona-Martínez, A.A.; Blanco, S.; Lebrero, R.; Muñoz, R. Innovative operational strategies in photosynthetic biogas upgrading in an outdoors pilot scale algal-bacterial photobioreactor. *Chemosphere* **2021**, *264*, 128470. [CrossRef] [PubMed]

37. Marín, D.; Ortíz, A.; Díez-Montero, R.; Uggetti, E.; García, J.; Lebrero, R.; Muñoz, R. Influence of liquid-to-biogas ratio and alkalinity on the biogas upgrading performance in a demo scale algal-bacterial photobioreactor. *Bioresour. Technol.* **2019**, *280*, 112–117. [CrossRef] [PubMed]

38. Silva, G.D.; Dlugogorski, B.Z.; Kennedy, E.M. Elementary reaction step model of the N-nitrosation of ammonia. *Int. J. Chem. Kinet.* **2007**, *39*, 645–656. [CrossRef]

39. Perez-Garcia, O.; Escalante, F.M.E.; De-Bashan, L.E.; Bashan, Y. Heterotrophic cultures of microalgae: Metabolism and potential products. *Water Res.* **2011**, *45*, 11–36. [CrossRef] [PubMed]